Locally pressed photonic crystal fiber interferometer for multiparameter sensing

Joel Villatoro,[1,2,*] Vladimir P. Minkovich,[3] and Joseba Zubia[1]

[1]*Department of Communications Engineering, Escuela Técnica Superior de Ingeniería (ETSI) de Bilbao, University of the Basque Country (UPV/EHU), Alda. Urquijo s/n, E-48013 Bilbao, Spain*

[2]*IKERBASQUE—Basque Foundation for Science, E-48011 Bilbao, Spain*

[3]*Centro de Investigaciones en Optica A. C., 37150, Leon, GTO, Mexico*

**Corresponding author: agustinjoel.villatoro@ehu.es*

Received February 19, 2014; revised March 25, 2014; accepted March 25, 2014; posted March 26, 2014 (Doc. ID 206826); published April 18, 2014

A mode interferometer consisting of a short section of photonic crystal fiber (PCF) fusion spliced to a standard single-mode optical fiber with localized perturbations is proposed for multiparameter sensing. In this sensing configuration, the parameter being sensed changes the visibility (an absolute parameter) of the interference pattern and also causes a shift (a relative parameter) to the interference pattern. To achieve this dual effect, a portion of the PCF is squeezed on localized regions with a serrated mechanical piece. In this manner, we introduce attenuation losses and effective refractive index changes to the interfering modes, hence, visibility changes and a shift to the interference pattern. Our device is suitable for monitoring diverse physical parameters, such as weight, lateral force, pressure, load, etc., with the advantage that compensation to temperature or power fluctuations is not required. Moreover, the sensor sensitivity can be adjusted in a simple manner.

OCIS codes: (060.2370) Fiber optics sensors; (060.5295) Photonic crystal fibers; (060.4005) Microstructured fibers; (280.4788) Optical sensing and sensors; (120.3180) Interferometry.

http://dx.doi.org/10.1364/OL.39.002580

Photonic crystal fibers (PCFs)—optical fibers comprising a pattern of microscopic voids present all over their length [1]—offer outstanding potential for the development of diverse kinds of sensors (see, for example, [2–4]). As demonstrated by several groups, most PCF sensors are sensitive to not only the parameter of interest (measurand), but also other parameters (e.g., temperature) that are likely to be present during their application [5–9]. In addition, PCF sensors may also be susceptible to drifts and noise induced by variations of the optical source or mechanical perturbations in the optical fibers and connectors. All these factors must be compensated; otherwise, they may be misinterpreted as measurand modulation. Therefore, in a practical situation, PCF sensors will require a compensation mechanism that may entail thermal isolation or additional reference sensors. To avoid these solutions, several groups have proposed different configurations to monitor two parameters simultaneously: typically, the parameter of interest and temperature. These solutions include, for example, a combination of PCF interferometers with long-period gratings [10–12] or Bragg gratings [13], or to infiltrate liquids of different indices into the PCF voids [14]. The disadvantage of most compensation mechanisms and configurations that combine two sensing methods is a certain degree of complexity of the sensor, which increases its cost. It is, therefore, important to devise new configurations or new solutions to overcome the cross sensitivity of PCF sensors without compromising their performance and main advantages, or increasing the overall cost.

Here, we introduce a PCF mode interferometer in which the parameter being monitored changes the visibility of the interference pattern, and also causes a detectable shift to the same. To achieve the dual effect in a simple manner, a PCF interferometer built via microhole collapse [15,16] was subjected to periodic localized pressure over a few millimeters with a serrated mechanical piece (see Fig. 1). The dual effect to the interference pattern was exploited to sense weight; however, the device can be used to sense diverse physical parameters, such as pressure, load, lateral force, etc. The advantage of the configuration proposed here is that temperature, power fluctuations, or mechanical perturbations in the optical fiber or connectors do not affect the measurements. In addition, the mechanisms to adjust the sensor sensitivity are really simple.

The PCF interferometer is sketched in Fig. 1 along with some details of its interrogation. The interferometer consists of a few centimeters of polymer-coated home-made PCF fusion spliced to a standard optical fiber (SMF-28). The short section of the single-mode fiber (SMF) spliced to the PCF at the distal end avoids contamination of the PCF voids, while the mirror ensures high reflectivity. The PCF used to fabricate our samples had an outer diameter of 125 μm, core diameter of 11 μm, average void diameter

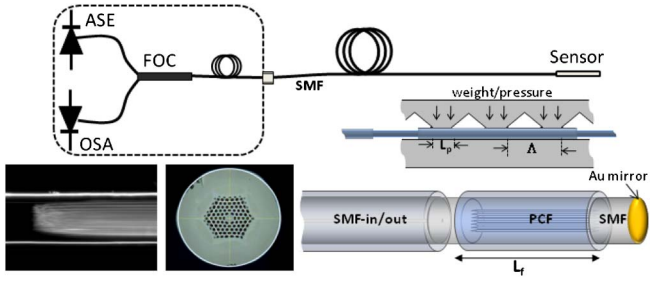

Fig. 1. Drawings of the PCF interferometer: schematic representation of its interrogation and illustration of the mechanical piece to apply localized pressure on the device. The micrographs show details of the PCF–SMF junction and the PCF cross section. ASE, amplified spontaneous emission; FOC, fiber optic circulator; SMF, single-mode fiber; OSA, optical spectrum analyzer. L_f is the interferometer (or PCF) length.

of 2.7 μm, and average void spacing (pitch) of 5.45 μm [17]. The fabrication of the interferometer is simple as it is carried out by means of the well-established fusion splicing technique. This ensures high reproducibility, robust devices, and low fabrication cost. During the splicing process, the voids of the PCF are intentionally collapsed over a region of ~200 μm in length. To achieve high-quality interferometers, both splices were carried out under identical conditions.

The outer diameters of the SMF and PCF are the same (125 μm), and the splicing process makes them to be aligned permanently. Therefore, there is axial symmetry in our device. On the other hand, the collapsed zones in the PCF cause a broadening of the propagating beam when it travels from the SMF to the PCF, or vice versa, and thereby, introduce a mode field mismatch between the fibers. The mode field mismatch combined with the axial symmetry and the modal properties of the PCF allows the excitation (and recombination) of modes that have similar azimuthal symmetry. The modes excited in the PCF have different effective indices (or different propagation constants), thus, they travel at different speeds. As a result, the modes accumulate a phase difference as they propagate along the length of the PCF. Therefore, if one launches light from a broadband optical source on the device and the output light is fed into an optical spectrum analyzer (OSA), the resulting reflection or transmission spectrum will exhibit a series of maxima and minima.

Figure 2 shows the reflection spectra at different weights of a 5.1 cm long interferometer squeezed with a serrated mechanical piece whose parameters were $L_p = 1$ mm and $\Lambda = 7.5$ mm. The spectra shown in Fig. 2 were obtained when calibrated weights were placed manually on top of the mechanical piece. It is important to point out that only 15 mm of the PCF were subjected to localized pressure because the rest of the PCF had no protecting coating as it was removed to splice the fibers. To ensure uniform compression of the interferometer and equilibrium of the mechanical piece, a stub of polymer-coated SMF was placed parallel to the PCF, at a distance of 2 cm. It can be noted in Fig. 2 that as

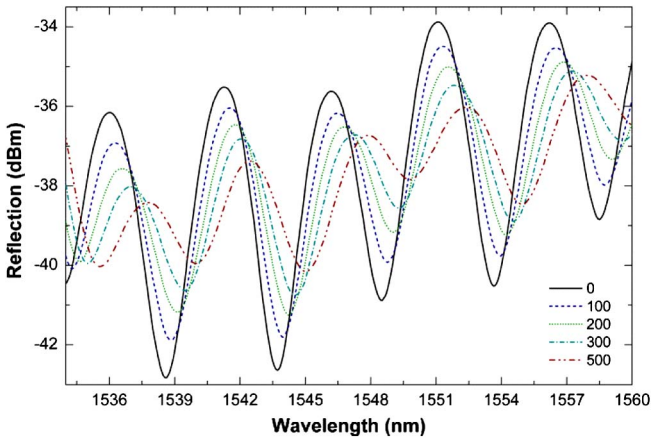

Fig. 2. Reflection spectra of a PCF interferometer for weight between 0 and 500 g. The mechanical piece that squeezed the interferometer had $L_p = 1$ mm and $\Lambda = 7.5$ mm. The length of the interferometer was 5.1 cm.

weight increases, the interference pattern shrinks and the shift of the interference pattern becomes more prominent.

To understand the origin of the two effects on the interference pattern, we need to analyze the effect of the localized pressure on the interfering modes. Let us suppose that two modes participate in the interference. In this case, the reflected intensity (I_R) can be expressed as

$$I_R = I_1 + I_2 + 2(I_1 \times I_2)^{1/2} \cos(\Delta\phi). \quad (1)$$

In Eq. (1), I_1 and I_2 are, respectively, the intensity of the two interfering modes, which in our case are a fundamental and a higher-order core mode as demonstrated in a previous work [18]. $\Delta\phi = 2\pi\Delta n L_f/\lambda$ is the total phase shift. $\Delta n = n_1 - n_2$, n_1 and n_2 being, respectively, the effective refractive index of the fundamental core mode and the higher-order core mode. L_f is the physical length of the PCF, or the length of the interferometer, and λ is the wavelength of the optical source. The visibility (V) of the interferometer can be defined as [19]

$$V = -10 \cdot \log_{10}[1-2(k)^{1/2}/(1+k)], \quad (2)$$

where $k = I_2/I_1$.

Now, if the PCF interferometer is subjected to localized pressure as shown in Fig. 1, then the interfering modes will lose power and their effective indices will change due to elasto-optic effects. Such effects are well documented in the literature (see, for example, [20,21]). In our case, the higher-order core mode is more sensitive to the external pressure and experiences a higher loss than the fundamental core mode. Therefore, the localized pressure on the PCF interferometer makes k to decrease, and, consequently, the interference pattern is compressed. $\Delta\phi$ also changes due to variations of Δn and makes the interference pattern to shift. This is the reason why the interference pattern is squeezed and shifts as the weight on the serrated mechanical piece increases. It is important to point out that the optical axis of the PCF is not bended during the measurements as it is supported on a flat surface (see Fig. 1). In this regard, our device is different from that reported in [22].

Figure 3 shows the changes in V of the interference pattern as a function of weight for two values of L_p (1 and 3 mm). The changes in visibility were measured from the obtained spectra by calculating the ratio of the difference over the sum of the absolute maximum and minimum of each spectrum. The changes in V are more prominent for the shorter L_p because the area of the PCF in contact with the mechanical piece is smaller, hence, the localized pressure is higher. The shift of the interference pattern as a function of weight for the case when $L_p = 1$ mm and $\Lambda = 7.5$ mm is shown in the inset in Fig. 3.

To analyze the role of V in the device sensitivity, we measured the transmission and reflection spectra of our interferometer for different weights. The visibility of our interferometer in the transmission mode was found to be lower than that in the reflection mode, which is consistent with the results reported in [19]. The changes in V measured for different weights when the

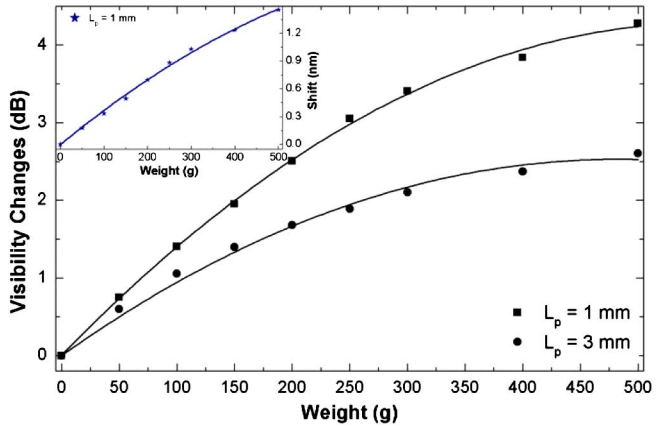

Fig. 3. Visibility changes as a function of weight observed in a 5.1 cm long PCF interferometer for two values of L_p. The inset shows shift of the interference pattern versus weight. In all cases $\Lambda = 7.5$ mm.

interferometer is operated in the transmission ($V = 4.25$ dB at 0 g) or reflection ($V = 8.52$ dB at 0 g) mode are shown in Fig. 4. It can be noted that sensitivity is higher when the visibility of the interference pattern is high.

The results shown in Figs. 3 and 4 suggest that the sensitivity of our sensor can be enhanced by simply reducing the value of L_p of the mechanical piece or by improving the visibility of the interferometer. Either of these alternatives does not increase the complexity of the device or its interrogation. An additional advantage of monitoring visibility changes is that they are easy to monitor as one only needs to find the maxima and minima of the interference pattern for which an inexpensive low-resolution OSA can be used. In addition, V is an absolute parameter and is immune to temperature fluctuations as demonstrated by several groups (see, for example, [23–25]). In fact, in our interferometer, temperature induces a shift to the interference pattern, but the intensity of the interfering modes, hence k and, consequently, V are not affected [18].

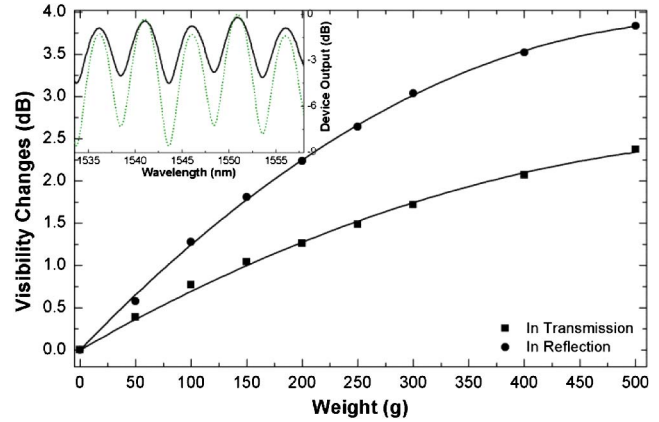

Fig. 4. Visibility changes as a function of weight observed when the PCF interferometer was operated in reflection and transmission modes. The inset shows the reflection (dotted line) and transmission (solid line) spectra when weight was 0 g. In all cases $L_p = 1$ mm, $L_f = 5$ cm, and $\Lambda = 7.5$ mm.

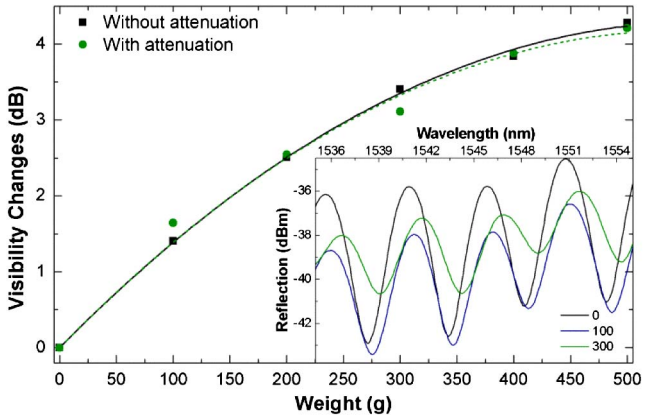

Fig. 5. Visibility changes versus weight observed in the PCF interferometer when no attenuation and high attenuation were introduced into the SMF. The inset shows the reflection spectra for a weight of 0 g without attenuation, 100 g with an attenuation of 2 dB, and 300 g with an attenuation of 1 dB. In all cases, the parameters were $L_f = 5$ cm, $L_p = 1$ mm, and $\Lambda = 7.5$ mm.

The effect of mechanical perturbations or attenuation losses on the performance of our devices was also studied as these can be a source of noise in intensity-modulated sensors. To do so, we introduced arbitrary attenuation losses in one connector and measured the spectra at different weights. Figure 5 shows the calibration curves that were obtained when no attenuation and attenuation were introduced. It can be noted that attenuation changes in our device have no significant effect on the sensor's response. The small deviation is attributed to the fact that the weights were not always on the same points on the mechanical piece as they were placed manually. Power fluctuations of the optical source did not affect the measurements either. This is so because visibility measurements are self-referenced, and thus, immune to fluctuations of the optical source.

In conclusion, a mode interferometer comprising a few centimeters of PCF fusion spliced at the distal end of a standard SMF and squeezed with a simple serrated mechanical piece is proposed for multiparameter sensing. The localized pressure on the PCF introduces attenuation losses and effective index changes in the interfering modes due to elasto-optic effects. As a consequence of the dual effect, the visibility of the interference pattern changes and it also shifts. Measurement of weight was demonstrated, but the configuration proposed here is suitable for sensing many other physical parameters, such as lateral force, load, pressure, impact, etc., as these will cause a dual effect on the interference pattern. To do so, probably, minor modifications on the sensor packaging will be necessary. The main advantage of the configuration proposed here include compactness, simplicity, low cost, immunity to noise induced by power variations of the optical source, and random attenuation in the optical fibers and connectors. In addition, it seems possible to adjust the sensor sensitivity by simply adjusting the length of the section that makes contact with the PCF or by enhancing the visibility of the interference pattern. We believe that the sensing configuration proposed here can be attractive to the fiber optic sensor community as it can be adapted for the development of new highly functional fiber optic sensors.

The authors acknowledge the financial support of the Spanish Ministerio de Economía y Competitividad under projects TEC2009-14718-C03-01, TEC2012-37983-C03-01, and TEC2013-46010-P, and also of the Gobierno Vasco/Eusko Jaurlaritza under projects AIRHEM-II and S-PE12CA001.

References

1. P. St. J. Russell, J. Lightwave Technol. **24**, 4729 (2006).
2. O. Frazao, J. L. Santos, F. M. Araujo, and L. A. Ferreira, Laser Photon. Rev. **2**, 449 (2008).
3. A. M. R. Pinto and M. Lopez-Amo, J. Sens. **2012**, 598178 (2012).
4. A. M. Cubillas, S. Unterkofler, T. G. Euser, B. J. M. Etzold, A. C. Jones, P. J. Sadler, P. Wasserscheid, and P. S. J. Russell, Chem. Soc. Rev. **42**, 8629 (2013).
5. C. Martelli, J. Canning, N. Groothoff, and K. Lyytikainen, Opt. Lett. **30**, 1785 (2005).
6. L. Rindorf and O. Bang, J. Opt. Soc. Am. B **25**, 310 (2008).
7. W. Shin, Y. L. Lee, B.-A. Yu, Y.-C. Noh, and T. J. Ahn, Opt. Commun. **283**, 2097 (2010).
8. H. Qu, T. Brastaviceanu, F. Bergeron, J. Olesik, I. Pavlov, T. Ishigure, and M. Skorobogatiy, Appl. Opt. **52**, 6344 (2013).
9. X. Xi, G. K. L. Wong, T. Weiss, and P. St. J. Russell, Opt. Lett. **38**, 5401 (2013).
10. Y. Zhou, W. Zhou, C. C. Chan, W. C. Wong, L.-Y. Shao, J. Cheng, and X. Dong, Opt. Commun. **284**, 5669 (2011).
11. Z. Wu, Y. Liu, Z. Wang, T. Han, S. Li, M. Jiang, P. P. Shum, and X. Q. Dinh, Appl. Phys. Lett. **101**, 141106 (2012).
12. D. J. J. Hu, J. L. Lim, M. Jiang, Y. Wang, F. Luan, P. P. Shum, H. Wei, and W. Tong, Opt. Lett. **37**, 2283 (2012).
13. S. Zhang, X. Dong, T. Li, C. C. Chan, and P. P. Shum, Opt. Commun. **303**, 42 (2013).
14. H. Liang, W. Zhang, P. Geng, Y. Liu, Z. Wang, J. Guo, S. Gao, and S. Yan, Opt. Lett. **38**, 1071 (2013).
15. J. Villatoro, V. P. Minkovich, V. Pruneri, and G. Badenes, Opt. Express **15**, 1491 (2007).
16. J. Villatoro, V. Finazzi, V. P. Minkovich, V. Pruneri, and G. Badenes, Appl. Phys. Lett. **91**, 091109 (2007).
17. V. P. Minkovich, A. V. Kiryanov, A. B. Sotsky, and L. I. Sotskaya, J. Opt. Soc. Am. B **21**, 1161 (2004).
18. G. Coviello, V. Finazzi, J. Villatoro, and V. Pruneri, Opt. Express **17**, 21551 (2009).
19. G. A. Cardenas-Sevilla, F. C. Fávero, and J. Villatoro, Sensors **13**, 2349 (2013).
20. A. Bichler, S. Lecler, B. Serio, S. Fischer, and P. Pfeiffer, J. Opt. Soc. Am. A **29**, 2386 (2012).
21. A. Sánchez, S. Orozco, A. V. Porta, and M. A. Ortiz, Mater. Chem. Phys. **139**, 176 (2013).
22. X. Yu and P. Shum, Proc. SPIE **6025**, 60250F (2006).
23. Z. L. Ran, Y. J. Rao, W. J. Liu, X. Liao, and K. S. Chiang, Opt. Express **16**, 2252 (2008).
24. C. Gouveia, P. A. S. Jorge, J. M. Baptista, and O. Frazão, IEEE Sens. J. **12**, 17 (2012).
25. B. Dong and E. J. Hao, J. Opt. Soc. Am. B **28**, 2332 (2011).